Ice Detector Measurements of Atmospheric Icing on a Cable

P. MCCOMBER
Ecole de Technologie Supérieure
4750, Henri-Julien
Montréal, Québec H2T 2C8, Canada

J. DRUEZ
Université du Québec à Chicoutimi
555, boulevard de l'Université
Chicoutimi, Québec G7H 2B1, Canada

M. ST-LOUIS
Hydro-Québec
855 est, Sainte-Catherine
Montréal, Québec H2L 4P5, Canada

ABSTRACT

Atmospheric icing is an important cause of damages to structures and power transmission lines in northern Quebec. An icing test line was set up on Mt. Valin (alt. 902 m) near Chicoutimi to measure icing loads on the type of stranded cables used on transmission lines. Measurements of icing loads on a 100 m span stranded cable are obtained from the cable end tension. An ice detector which counts icing detection alarm cycles per unit time is used to measure the icing intensity. Average wind speeds, directions and temperatures at the study site were also recorded.

A detailed study of a few icing events was made in order to relate the icing rate, as measured by the ice detector, with the cable icing rate. Two types of icing events can be distinguished from the range of the ice detector data. Freezing precipitation is associated with significantly higher icing intensities than cases in which only in-cloud icing occurs. Different calibration curves for icing rates of the ice detector were developed to predict cable icing for these two types of events.

The cable icing rate is derived by taking into consideration the accretion size, wind direction and collection efficiency. Results indicate that in most events, the ice detector data can be used to predict ice loads on transmission line cables with an average error of only 2.6 percent per hour. Predictions are generally more accurate at lower icing rates.

INTRODUCTION

Atmospheric icing is an important cause of damages to stuctures and power transmission lines in northern Québec. Due to the topography, it is not possible for the power transmission lines to reach the southern markets without going through mountains for substantial distances. In these mountains, clouds are frequently found above a altitude of 300 m (984 ft) and in-cloud icing will occur with increasing frequency above that altitude and is therefore a hazard for the transmission lines.

Measurements of atmospheric icing on power transmission lines have been made to study the frequency and severity of rime loads (Diem, 1956). Field measurements have been obtained by instrumenting experimental cables located in areas where icing is frequent (Govoni and Ackley, 1983; McComber and Govoni, 1985; Smith and Barker, 1983; Druez et al., 1988).

In order to study in-cloud icing, a test cable was set up on Mt. Valin at an altitude of 902 m (2959 ft), in the Laurentian mountains near Chicoutimi. This test facility consists of a 96.5 m (316.5 ft) cable which was designed and built in collaboration with Hydro-Québec to investigate icing of power line cables. This installation provided the opportunity to gather cable icing data for complete winter seasons. At the Mt. Valin test site, as long as the temperature remains below 0°C, rime accretes and a significant portion stays on the line during the winter season until it melts in the spring. However, it is difficult to relate cable icing measurements to a standard icing meteorological parameter. Icing has never been systematically measured, as precipitation for example, by the meteorological services. Tattelman (1982) has shown that an ice detector can fill that need at least until a better instrument can be marketed.

The purpose of this study is to analyze icing data collected on a test cable and correlate the accreted mass of ice with measured ice detector signals in order to better understand this complicated phenomenon, to contribute to the development of an improved icing model for power transmission line cables, and to verify the possibility of using the ice detector to predict cable icing.

TYPES OF ATMOSPHERIC ICING AFFECTING STRUCTURES

Three basic kinds of ice are formed by accretion in the atmosphere: glaze, hard rime and soft rime. Glaze is transparent and it has a density with respect to water of approximately 0.9 (the density of pure ice is 0.917). Hard rime is white and sometimes opaque, depending on the quantity of air trapped inside the ice. Its density varies from 0.6 to 0.9. Soft rime is white and opaque. It is feathery or granular in appearance with a density less than 0.6. The density will increase with increasing drop size, temperature, windspeed and liquid water content.

Cloud or fog droplets have diameters smaller than 200 μm. Cloud droplet sizes measured experimentally indicate that low level clouds, which can affect a structure on a mountain summit, have droplet sizes in the 1-45 μm range. Consequently, exposure to supercooled clouds or fog will usually result in soft rime. On the Mt. Valin summit in-cloud icing is frequent from December through March. However freezing precipitations, which have droplets larger than 200 μm, also occur and are most frequent in early winter. The higher liquid water content associated with the precipitations can produce hard rime. The boundary between in-cloud and freezing precipitation icing is difficult to establish on a mountain icing site where clouds and precipitations are often mixed and where the icing obtained varies in density, covering the range from soft to hard rime.

EXPERIMENTAL INSTALLATION

The cable icing site is located at the summit of Mt. Valin, in proximity to a Radio-Québec communication antenna which serves the Saguenay-Lac St-Jean area. The presence of the Radio-Québec antenna and its associated access and services combine to make this particular well-exposed summit in the Laurentian mountain range an excellent location for this study.

The experimental installation is composed of a test cable, a thermistor, a de-iced anemometer and an ice detector. A 96.5 m (316.5 ft) span test line supports the 35 mm (1.38 in.) diameter stranded cable which was used to collect the icing data analyzed in this report. A schematic diagram of this cable is shown in Fig. 1. The stranded cable has one of its ends 0.37 m lower than the other. This difference was found when accurate level measurements were made after cable installation. However this difference is only 0.4 % of the span and therefore does not significantly change the equal distribution of weight between the supports.

Load cells measure the cable end tension (N) which is then converted to icing mass per unit length (kg/m), after accounting for the geometry of the cable and line (McComber et al., 1987). Data is collected by an acquisition system installed with signal conditioners in a building close to the experimental test line. The ice is assumed to be

uniformly distributed on the cable span and the icing mass per unit length is obtained from the vertical component of the measured tension using the initial cable angle at the support. This angle, shown in Fig. 1 for the test cable, was measured accurately with surveying instrumentation.

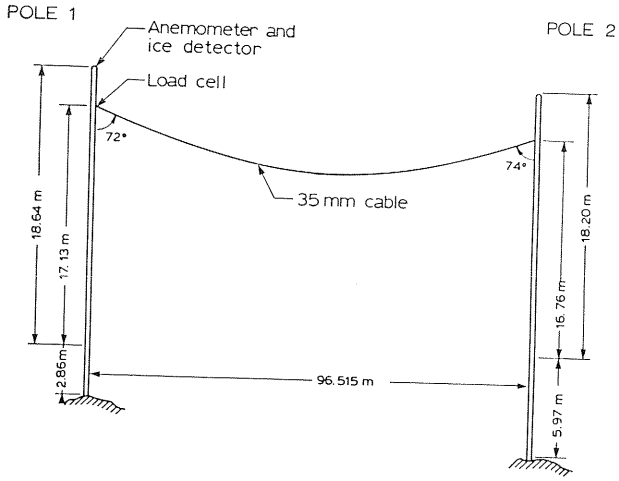

Fig. 1. Schematic diagram showing dimensions of the test cable.

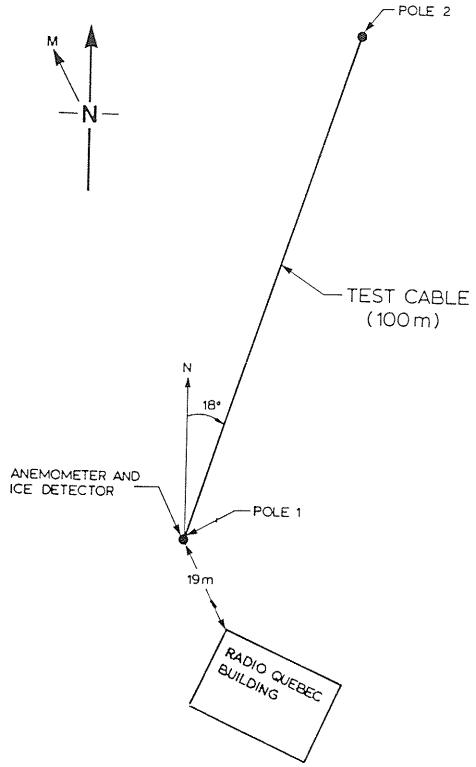

Fig. 2. Direction of the test cable.

Data are collected at 30 min intervals and include the computed average of 180 samples, i.e. every 10 s, for the load cells, 50 samples for the wind velocity and one sample for the temperature and the ice detector. During the icing season, data are transmitted via a telephone line to a computer in the university laboratory and are verified to prevent transmission errors. Each month, curves of the measured icing parameters are plotted. From the measured end tension in the cable, an equivalent average ice load M expressed as a mass per unit length (kg/m), is calculated.

An equivalent ice-covered cable diameter D in meters is often used to describe ice accretion size. The average ice load M can be converted to equivalent diameter by:

$$D = 2\left[\frac{M}{\rho\,\pi} + \frac{D_b^2}{4}\right]^{1/2} \qquad [1]$$

where D_b is the bare cable diameter and ρ is the accretion density (kg/m^3)

In Figure 2, the orientation of the test cable is shown. This orientation is important when determining the effect of the wind speed on ice accretion.

INSTRUMENTATION AND MEASUREMENTS

The ice detector

An ice detector (GENEQ, IREQ-1000) records the occurence and duration of icing conditions. This type of ice detector was originally developed to detect ice formation in the intake portion of turbomachinery. These detectors were aerodynamically designed for use on aircraft, but they have also been used to detect icing on towers. The ice detector's operation is based on the magnetostriction principle. An oscillator forces a small closed cylinder (the sensing probe) to vibrate longitudinally, parallel to its axis. It is driven at its resonant frequency when dry, but accretion of ice will cause a shift in resonance corresponding to the increase in ice adhering to the probe. After a small preset thickness of ice has accumulated, the sensor is de-iced by heating. The sensing probe used by GENEQ is a Rosemount 871 cylinder, 6.2 mm in diameter and 25.5 mm long. Tattelman (1982) has concluded that such a detector has presently the greatest potential as a meteorological instrument for the detection of icing. However, he had also pointed out that the major hindrance to utilization of the detector "off the shelf" for making icing observations, is the problem of retention of melt water on the flat surface area on top of the strut on which the sensor is located. This retained water can cause erroneous cycling upon refreezing. This problem has been alleviated, at least partly, for the GENEQ instrument in use on Mt. Valin by a redesign of the supporting strut made by Hydro-Québec IREQ. The strut is bent sideways by mechanical action permitting any melt water to be removed from the instrument between cycles. A photograph of the ice detector is shown in Fig. 3.

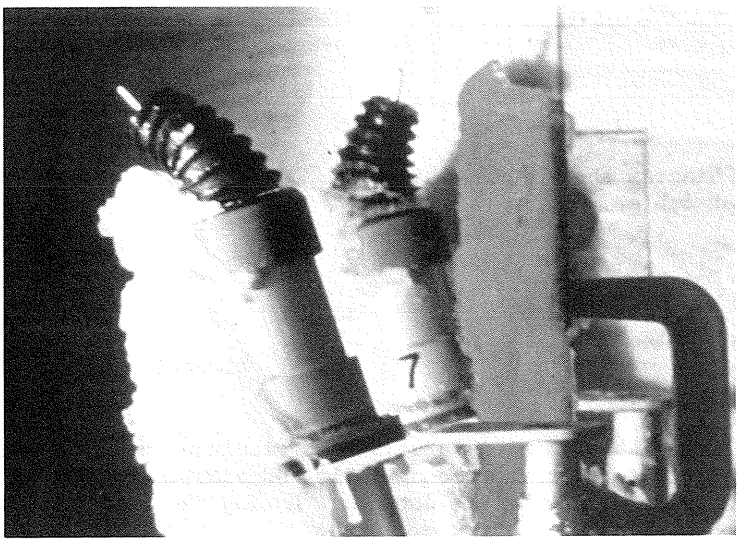

Fig. 3. Photograph of the ice detector.

De-iced anemometer

The wind velocity magnitude and direction are measured with a de-iced anemometer (HYDROTECH). The anemometer has a heated rotor (WS-3) and a heated direction vane (WD-3). Knowing the line orientation, the wind velocity component normal to the test cable is computed.

Ice detector calibration

Tattelman (1982) has made an extensive study on the calibration of the ice detector. In his calibration, the distinction is made between freezing rain and in-cloud icing. Since there is a significant difference in droplet size and therefore in the collection efficiency of the obstacle, this distinction will be retained in the present work.

In the case of in-cloud, icing his results were obtained for cylinders of various diameters and 300 mm in length, and summarized in interpolated curves giving the mass of ice, M (kg/m), as a function of the number of detector alarms, x. This calibration curve can be interpolated for the Mt. Valin 35 mm cable, and divided by 0.3 to obtain icing on a 1 m cable:

$$M = 0.0377 + 0.0075\ x \qquad [2]$$

In Eq. (2) there is a small ordinate (0.0377), such that repeated use of this curve for a small number of alarms would result in an unacceptable multiplication of an error. This is not appropriate, if this equation is to be used, to find an icing rate from a small alarm cycle rate. To obtain the same accuracy using repeatedly a small number of cycles, a curve with a zero ordinate was derived:

$$M = .00867\ x \qquad [3]$$

Eq. (3) was obtained by minimizing the surface between the straight line given by Eq. (2) and a line of unknown slope passing through the origin. The minimization of the error was done between 0 and 50 cycles. The original calibration curve corresponding to Eq. (2) and the curve passing through the origin are shown in Fig. 4.

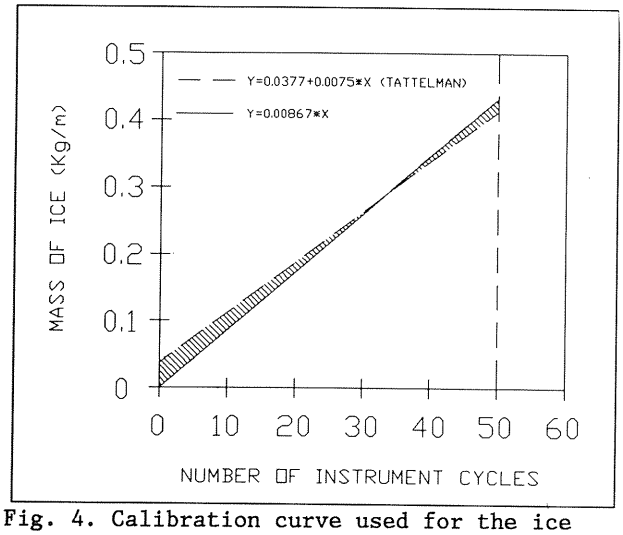

Fig. 4. Calibration curve used for the ice detector, in-cloud icing.

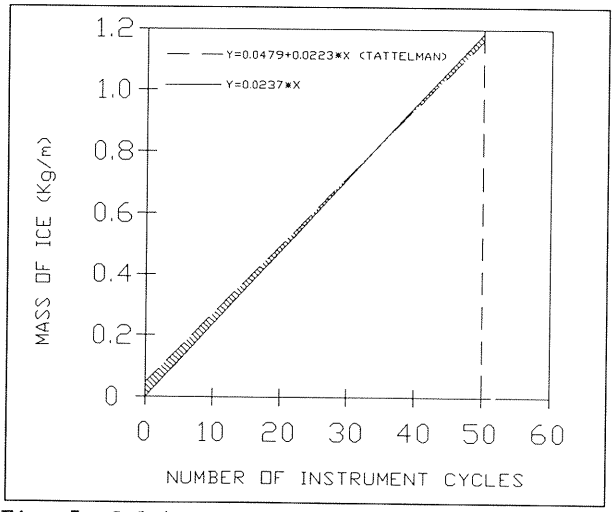

Fig. 5. Calibration curve used for the ice detector, freezing rain.

This equation can also be applied to find the icing rate from the detector cycle rate:

$$\delta M = .00867\ \delta x \qquad [4]$$

The calibration curve given by Tattelman (1982) for freezing rain, multiplied by the appropriate constants for a 35 mm cable and 1 meter in length:

$$M = 0.0479 + 0.0223\ x \qquad [5]$$

and the optimum straight line passing through the origin and obtained by the same method, is:

$$M = .0237\ x \qquad [6]$$

Figure 5 shows these two calibration lines given by Eqs. (5) and (6). Equation (6) will be used below to predict cable icing in the case of freezing precipitation.

Cable icing rate

The icing intensity expressed as mass per unit area and unit time is given by (Makkonen, 1984; Horjen,1983) :

$$R = E\ w\ V_n \qquad (\ kg/m^2s) \qquad [7]$$

where E is the dimensionless collection efficiency, w is the liquid water content (kg/m^3) in the air flow and V_n is the normal wind velocity (m/s). The collection efficiency is defined as the ratio of the mass of drops impinging on an object in unit time to the mass of drops that would have impinged in the same time if there were no deflection resulting from moving air around the cable.

To obtain the accreted mass in 1/2 hour at time t_i, δM_i, the icing intensity is multiplied by the obstacle cross-section normal to the flow direction and the time interval δt. For a cable, if D (m) is the equivalent cable diameter, Eq. (1):

$$\delta M_i = E\ w\ V_n\ D\ \delta t \qquad [8]$$

In order to be able to use the ice detector calibration curves to predict the icing rate of the cable, the effect of three variables must be considered. These are the normal wind speed, V_n, which will have the same effect for in-cloud icing and freezing precipitations, the collection efficiency, E, and the equivalent accretion diameter D.

In-cloud icing

For in-cloud icing, the droplets are small and the collection efficiency can influence the icing rate. However, at low wind speed, experimental data has shown that the calculated collection efficiency is unreliable. McComber et Govoni (1985) and Personne (1988) have shown that a modified collection efficiency has to be used in order to take into account the effect of the accretion surface roughness on the collection efficiency. The value of the calculated collection efficiency E_{oc} has therefore to be corrected using an expression suggested by Personne (1988) and based on experimental results:

$$E_o = E_{oc} + 2.03\ (1 - E_{oc})\ D_o \qquad [9]$$

where E_{oc} is the initial calculated collection efficiency and D_o the initial equivalent diameter of the accretion. Using this value, the icing rate was corrected both for the collection efficiency and the initial accretion size:

$$\delta M_i = 0.0867\ \delta x\ C_E \quad \text{where} \quad C_E = E_o\ D_o\ /\ E_b\ D_b \qquad [10]$$

E_b and D_b are the collection efficiency and diameter of the bare cable respectively.

The following expression was used to find the resulting ice mass as a function of time:

$$M_i = M_{i-1} + \delta M_i \qquad [11]$$

Freezing precipitations

For freezing precipitations, i.e. for droplet with d > 200 μm, which is the case for freezing rain, the collection efficiency E is equal to 1 even for low wind speed, and hence is not considered in the calculations. The icing rate, δM_i, is given by:

$$\delta M_i = 0.0237\ \delta x\ (D_{i-1}/D_b) \qquad [12]$$

The equivalent diameter D_{i-1} is found using Eq. (1), assuming a cylindrical ice accretion shape and an accretion density of $\rho = 900\ kg/m^3$. In this case the higher icing rate justifies a calculation of the equivalent diameter D_{i-1} at every time step.

Wind intensity and direction

The wind velocity is measured by an anemometer located on top of pole 1 of the test line (Fig. 1). Wind velocities vary with height from ground level. This variation is usually assumed to be in the form of a power law (Blevins, 1977):

$$\frac{V(z)}{V(L)} = \left[\frac{z}{L}\right]^{\alpha} \qquad [13]$$

where the velocities at different heights from ground z are compared with the velocity at a reference height L. For the type of terrain where the test line is located, the exponent α should be approximately 0.28 (Blevins, 1977). The ratio of velocities of cable heigth to ice detector height is 0.975 which is approximately unity and has not been taken into consideration for the computation of cable icing.

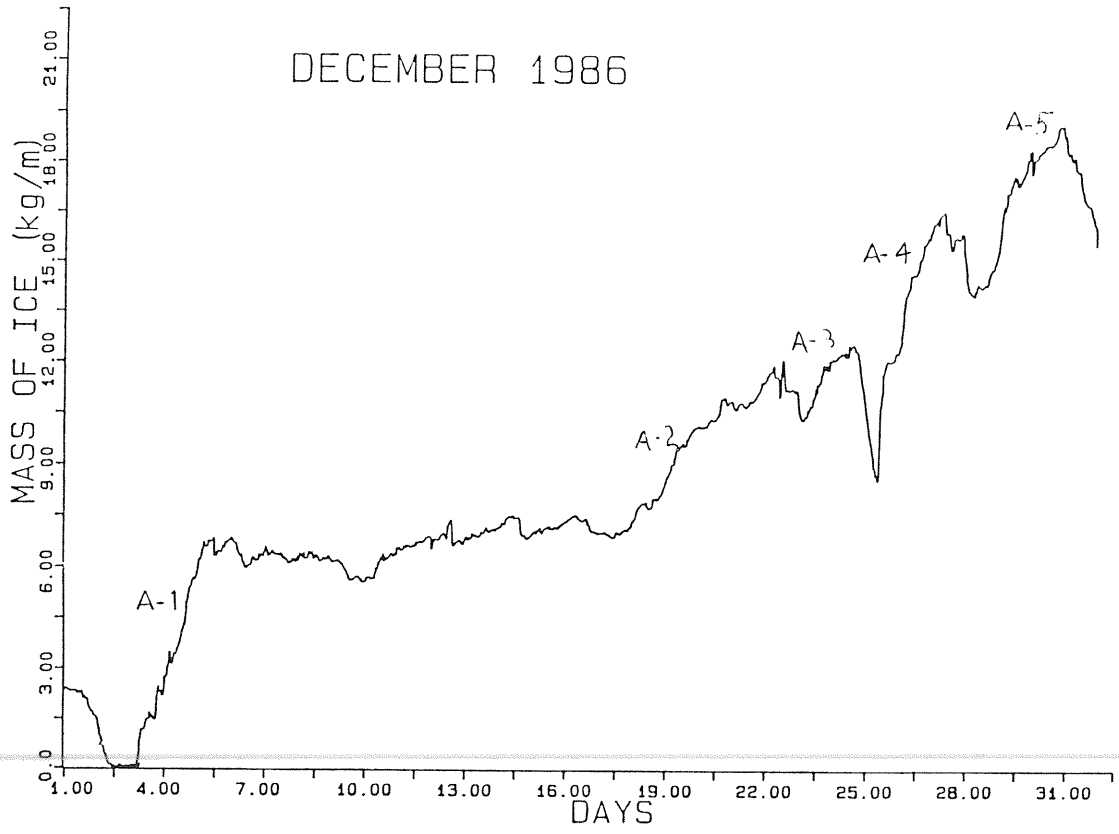

Fig. 6. Mass of ice accreted on the 35 mm cable in December 1986.

Equations (10) and (12) are for a cylinder or cable perpendicular to the wind direction. If the are not perpendicular, the icing rate, δM_{ic}, must be corrected by:

$$\delta M_{ic} = \delta M_i \cdot \cos \Theta \qquad [14]$$

where Θ is the angle between the wind direction and the direction normal to the cable.

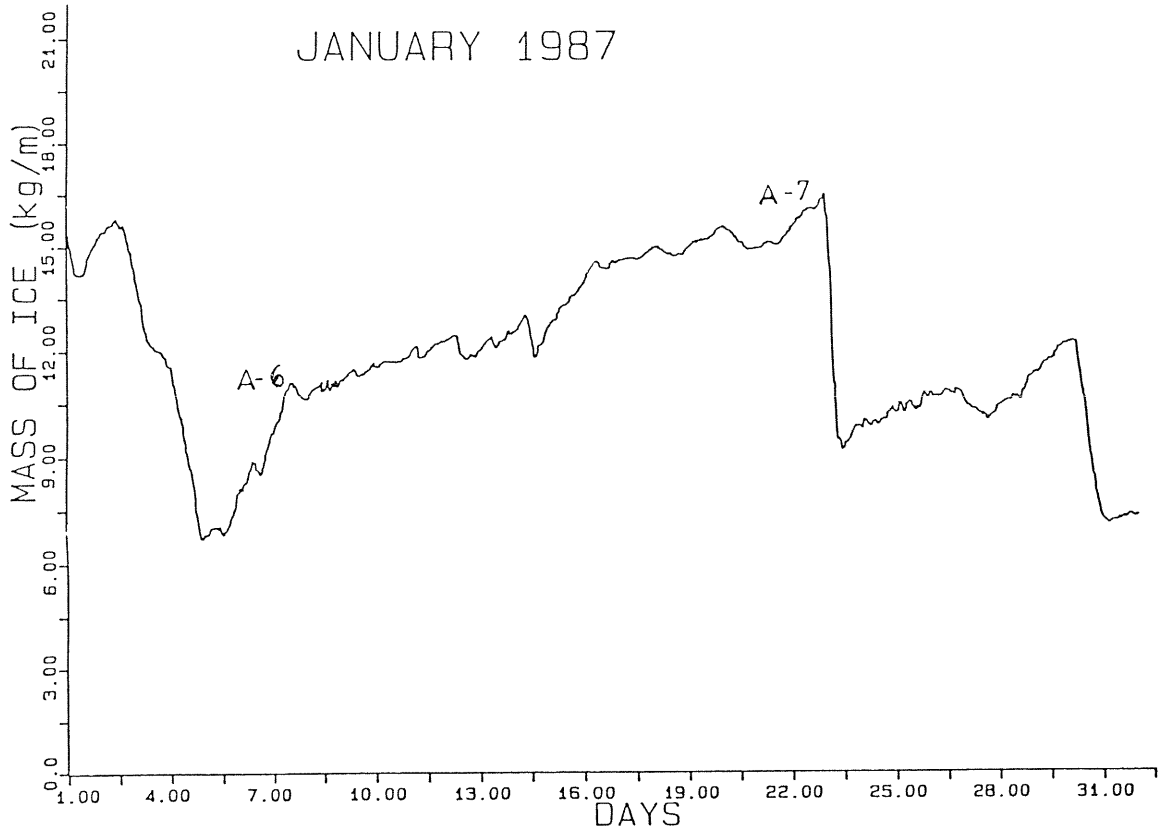

Fig. 7. Mass of ice accreted on the 35 mm cable in January 1987.

RESULTS AND DISCUSSION

Icing measurements

Icing data from the 1986-87 icing season were analyzed. This data period was chosen because important icing events were recorded and the instruments performed adequately. A certain number of accretion events have been chosen in December and January on the basis of the number of icing alarms in an hour and are indicated in Figs. 6 and 7. Whenever the icing alarm rate was more than two or three alarms per hour for four consecutive hours, the icing period was considered as a separate event.

The seven (7) accretion events studied are summarized in Table 1 and are shown in Figs. 8 to 14. From the measurements taken it is not as easy to make the distinction between freezing rain, where precipitation and large droplets are present, from in-cloud icing where only smaller droplets are involved. Freezing precipitations are recognized when an icing rate of approximately 0.4 kg/m.h is obtained for the cable during an event. However this icing rate is not usually sustained for the complete event. In Table 1 the average icing rate during each event is shown and the events classified as freezing rain have approximately twice the icing rate (0.19 kg/m.h) measured for in-cloud icing events (0.099 kg/m.h).

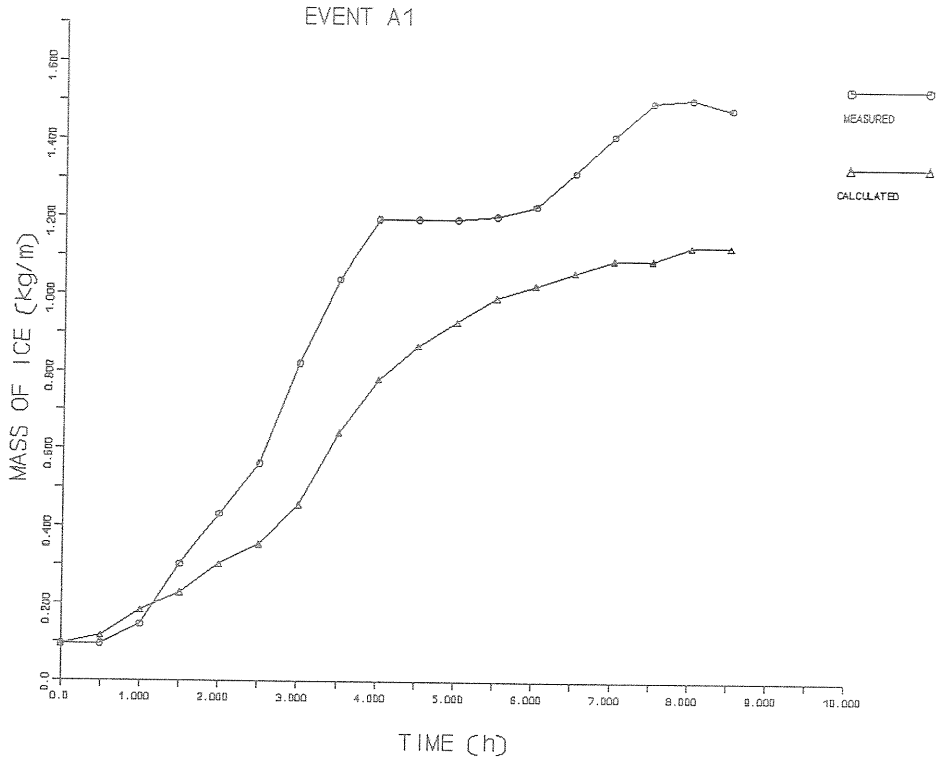

Fig. 8. Comparison of the mass of ice measured on a cable with the mass predicted by the ice detector, event A-1.

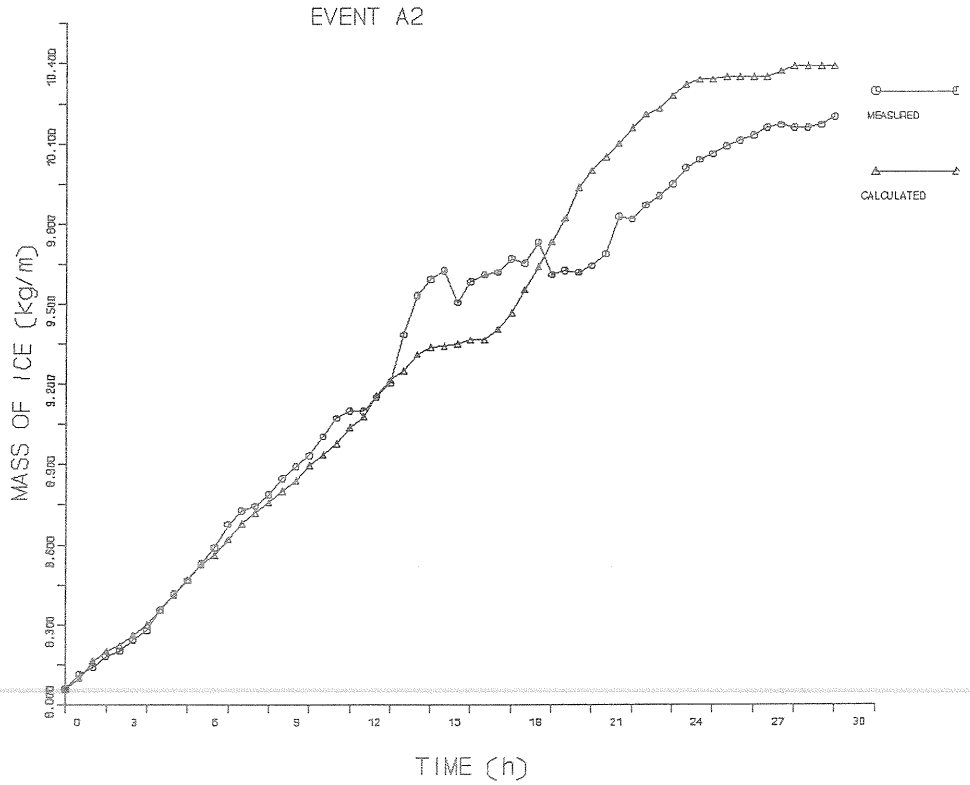

Fig. 9. Comparison of the mass of ice measured on a cable with the mass predicted by the ice detector, event A-2.

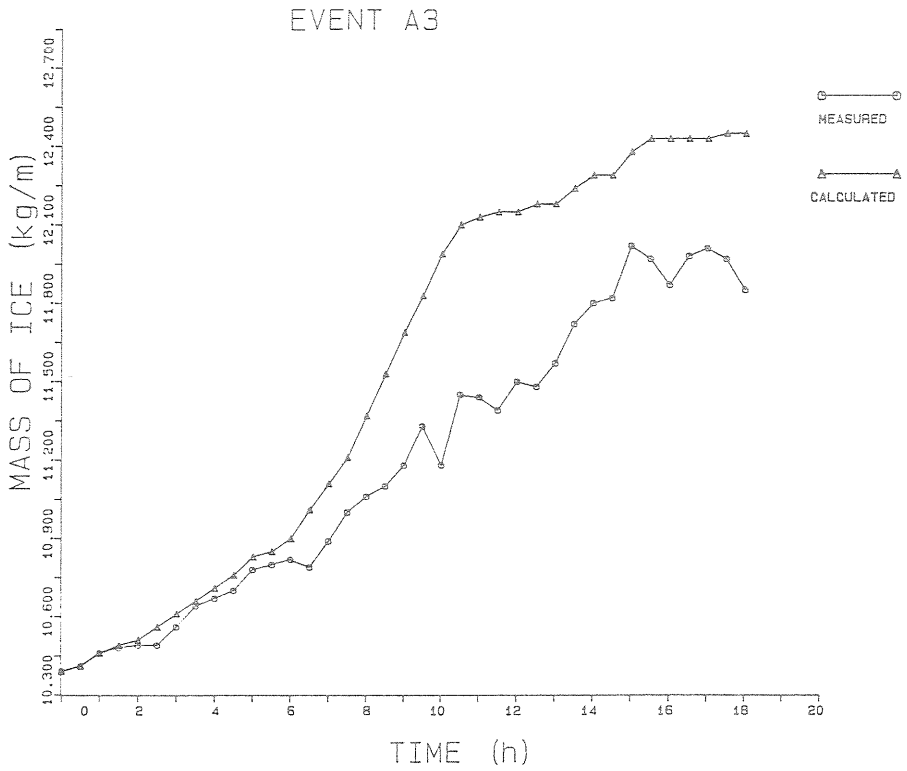

Fig. 10. Comparison of the mass of ice measured on a cable with the mass predicted by the ice detector, event A-3.

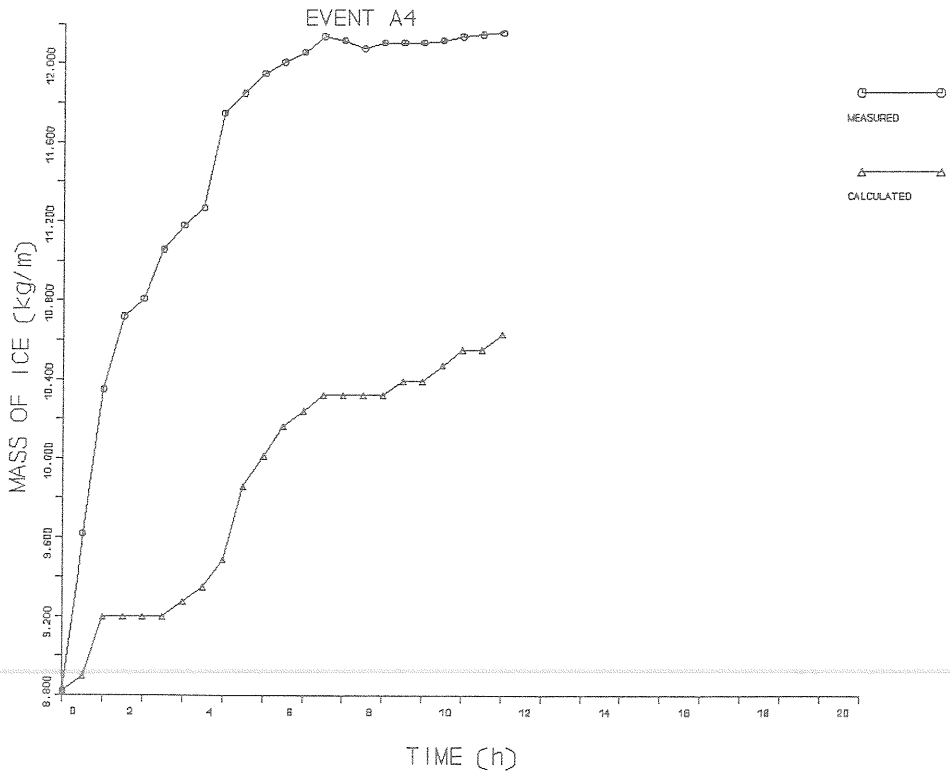

Fig. 11. Comparison of the mass of ice measured on a cable with the mass predicted by the ice detector, event A-4.

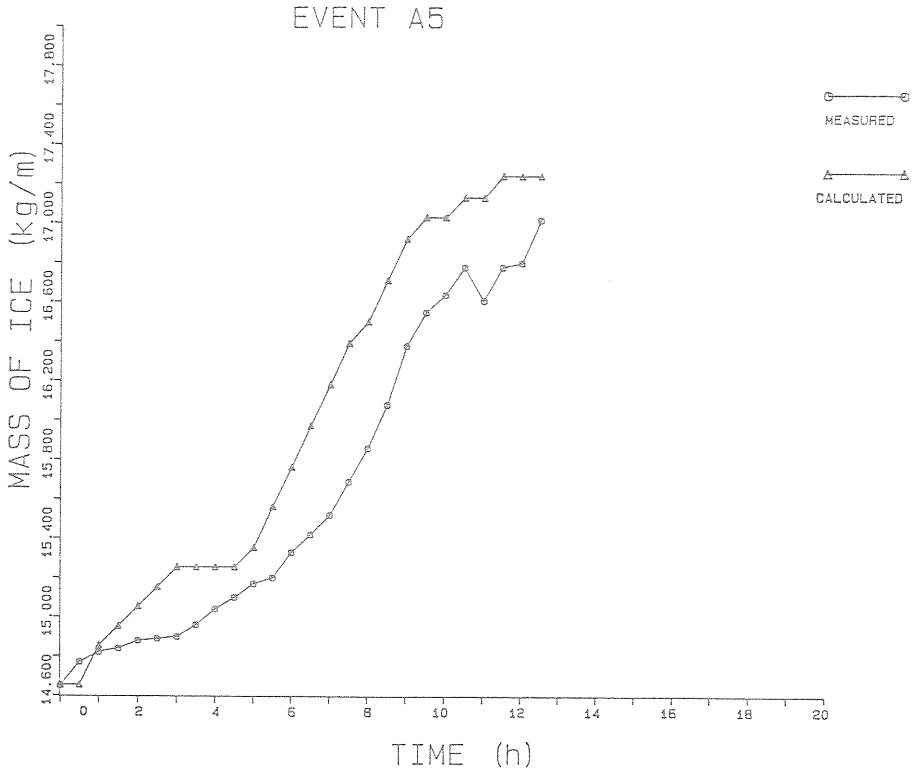

Fig. 12. Comparison of the mass of ice measured on a cable with the mass predicted by the ice detector, event A-5.

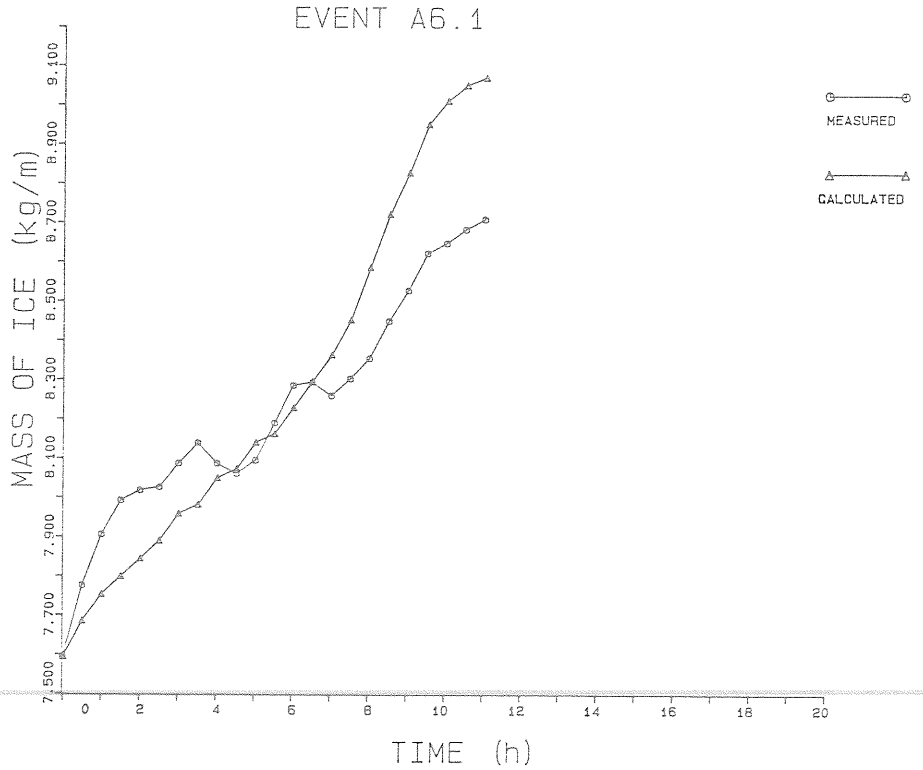

Fig. 13. Comparison of the mass of ice measured on a cable with the mass predicted by the ice detector, event A-6.1.

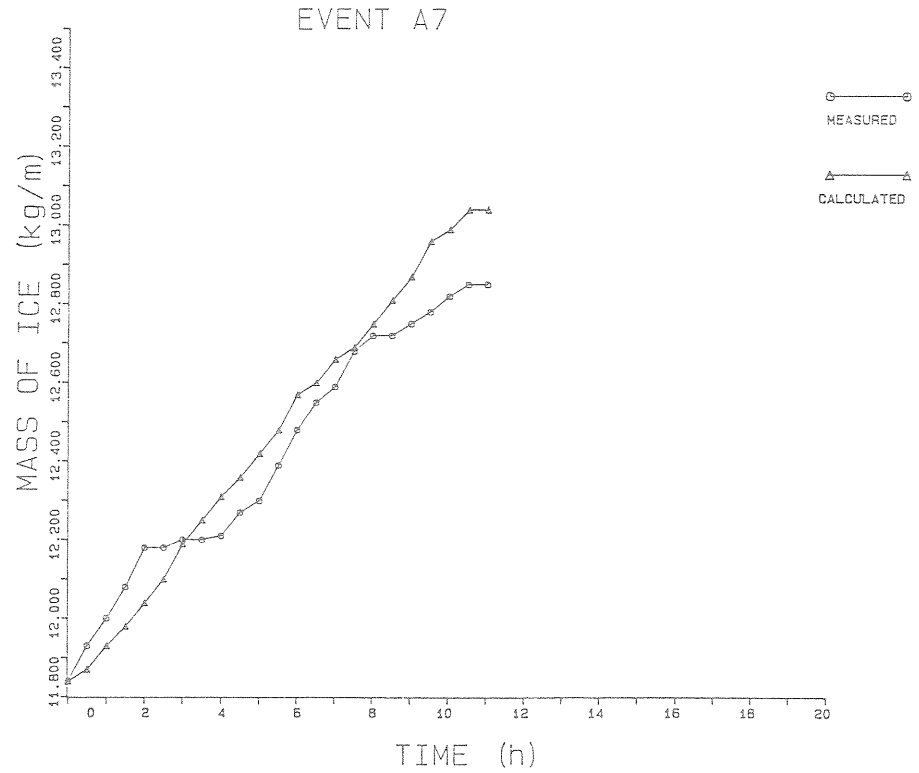

Fig. 14. Comparison of the mass of ice measured on a cable with the mass predicted by the ice detector, event A-7.

Table 1

Summary of icing events

Event number	Date and time	Duration (h)	Average icing rate (kg/m.h)	Average error(%/h)
A-1	3 Dec 4:30	8.5	0.14 (FR)	- 2.5
A-2	18 Dec 19:30	28	0.078	+ 0.3
A-3	23 Dec 3:30	18	0.098	+ 1.9
A-4	25 Dec 9:30	11	0.23 (FR)	- 5.4
A-5	28 Dec 17:30	12.5	0.20 (FR)	+ 0.7
A-6.1	5 Jan 22:00	11	0.12	+ 2.5
A-6.2	6 Jan 15:00	8	0.1	- 9.9
A-7	14 Jan 15:30	11	0.1	+ 1.6
			Average absolute error (%/h):	2.6

In-cloud icing

In Table 1 events A-2, A-3, A-6 and A-7 are classified as in-cloud icing. During event A-6 a significant amount of ice was shedded over a short period of a few hours. Hence that period was removed from the analysis and the remaining time separated in two parts: A-6.1 and A-6.2. Not including event A-6.2, the average absolute difference between the accretion mass predicted and measured is 1.6 %/h. In the case of event A-6.2, the predicted ice mass falls well below the mass collected by the cable. There are two possible explanations for this difference. The first cause could be the change in weather conditions during the analysis period. The change from supercooled droplets to wet snow particles would increase the accretion mass even though the ice detector would not react

to wet snow. The second possibility could well be a temporary failure of the detector, as observed in the case of freezing rain and explained below in the discussion of these events. Indeed the high average icing rate measured in event A-6.2 (0.12 kg/m.h) is the highest among events classified as in-cloud icing and could have been responsible for a partial failure of the ice detector.

Results also show that the ice detector signal increases regularly whereas the accretion mass signal shows more irregularities. The ice detector signal measures a number of icing alarms in a given time period and must always be increasing whereas the measured ice mass on the cable can be affected by ice shedding that most probably occurs in certain wind conditions but that the detector is unable to predict.

In summary, there is a fairly good agreement between the icing rate predicted by the ice detector and the icing rate measured. The average error for the four events studied is 1.6 %/h. However, since the total mass is obtained by an integration over the event period, a small error in the icing rate predicted will result in a large difference in mass over a long period. The longest event, A-3, has a difference of 34 % between the calculated and measured mass for the 28.5 h period.

Freezing rain event

Events A-1, A-4 and A-7 are classified as freezing rain, based on their higher icing rate. This is to be interpreted as the probable presence of freezing precipitations during part of the event. However in-cloud icing is likely to occur simultaneously, and precipitations can also be absent in part of the period studied. Results for these three events show a larger error, an average of 2.9 %/h difference between calculated and measured average icing rate.

At these higher icing rates, the detector has failed at least during part of each event. In the case of event A.1 the ice detector became completely surrounded by the accretion and failed to record icing after 8.5 h. Only the initial period of the event, when the detector was working was considered for the comparison. In the case of events A-4 and A-5 the ice detector recorded no alarms for a pediod of two hours and then seemed slow to record strong icing in the recovery period. It has been observed in the field that the mechanical movement of the ice detector which was intended to remove water from melted ice on the probe is also effective in breaking some of the ice forming on the strut. However, this is not equally effective depending on the wind direction. If the wind is at 180^{o} with the inclining angle, then the movement is less effective in breaking the ice forming in the opposite direction on the strut and hard rime can accrete in the back of the instrument up to a point where the droplets are prevented from reaching the probe. This is the type of failure observed in event A-1, and this is most probably what happened during events A-4 and A-5. Indeed even if the detector probe operates in the vertical direction in order to be insensitive to the wind direction, its mechanical movement, in a preset direction, makes the response of the instrument dependent on the wind direction for high icing rates.

In summary, the analysis of these icing events shows that the number of ice detector alarm cycles per unit of time can be used with appropriate calibration curves to predict the cable icing rate with reasonable accuracy. However, additional factors will affect the total icing rates on the cables. Improvement in modeling cable icing should include the effect of cable diameter (McComber et al., 1987) which controls torsional stiffness of the cable and finally dynamics of the cable during icing. The ability of the ice detector to predict icing rate is therefore dependent on the continued improvements of cable icing modeling. Also since the atmospheric icing phenomenon is highly history dependent, ice shedding appears to be a variable which has to be included in order to make an accurate prediction of cable icing in mountains. Because of the many time dependent variables involved and the complexity of cable icing, more data for different cable sizes and heights, must be collected and analyzed to establish an adequate empirical model. The cable icing model will in turn permit the narrowing of the gap between the icing intensity as measured by the ice detector and the ice mass actually accreting on the cable.

CONCLUSIONS

A relationship was established between ice load measurements obtained on a single cable and an ice detector signals for December 1986 and January 1987, at Mt. Valin. The ice detector number of alarm cycles was counted for half hour periods and used as a measure of icing rate on the instrument, leading to a prediction of the ice mass accreting on the cables. The effects of the wind direction, collection efficiency and accretion size are included in the calculations of the predicted cable icing. The events analyzed indicate that the ice detector performed adequately when the icing rate was less than 0.2 kg/m.h for which an average error of 2.6 %/h was verified. Future improvements in the modeling of cable icing will increase further the accuracy of cable icing prediction with the ice detector.

ACKNOWLEDGMENTS

The Mt. Valin test line was built and instrumented as part of a contract from Hydro-Québec (HO 924345). This work was also supported by the Natural Sciences and Engineering Research Council of Canada. The authors thank Radio-Québec for the permission to use the Mt. Valin building and Hydro-Québec for their help in reaching the site during the winter months. The following people have contributed to the testing: Bernard Desbiens, Serge Gauthier and Alain Royal.

REFERENCES

Blevins, R. D. 1977. " Flow-Induced Vibration", Van Nostrand Reinhold, Co., New-York, pp. 164-182. Reprinted in 1986, Robert E. Krieger, Malabar, Florida.

Diem, M. 1956. "Ice Loads on High Voltage Conductors in the Mountains", Archiv fur Meteor., Geophys. und Bioklim., Vol B7, pp. 84-95. (in German)

Druez, J., McComber, P., Félin, B. 1988." Icing rate Measurements made for different cable configurations on an icing Test Line at Mt. Valin", 4th International Workshop on Atmospheric icing of Structures, Paris, Electricité de France, special Report, pp. 124-128.

Govoni, J.W., Ackley, S. F. 1983. " Field Measurements of Combined Icing and Wind Loads on Wires". Proceedings of First International Workshop on Atmospheric Icing of Structures, CRREL Special Report 83-17, pp 205-215.

Horjen, I. 1983, "Icing on Offshore Structures- Atmospheric Icing", Norwegian Marine Research No 3, pp. 9-22.

Makkonen L., 1984. " Modelling of Ice Accretion on Wires", J. of Appl. Meteor, Vol 23, pp. 929-939.

McComber, P., Druez, J., Bouchard, D., Falgueyret, A. 1987. "Atmospheric Icing Load Measurements on a Cable Using the End Tension", Cold Reg. Sc. and Techn., Vol 13, pp. 131-141.

McComber, P., Govoni, J.W. 1985. "An Analysis of Selected ice Accretion Measurements on a Wire at Mt. Washington", Proceedings of the 42nd Eastern Snow Conference, pp. 34-43.

Personne P., 1988, " Effet de la rugosité sur la croissance du givre à faible vitesse: Résultats expérimentaux et modèlisation ", Thèse de doctorat, Université Blaise Pascal, Clermont-Ferrand, 231 pp.

Smith, B.W., Barker, C.P. 1983. "Icing of Cables", CRREL Special Report 83-17, pp 41-49.

Tattelman, P. 1982. "An Objective Method for Measuring Surface Ice Accretion", J. of Applied Meteor., Vol 21, no 4, pp. 600-612.